Accepted Manuscript

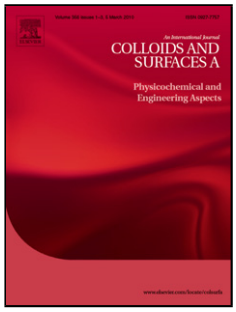

Title: Preparation and properties of a magnetic field responsive three-dimensional electrospun polymer scaffold

Author: Angela Jedlovszky-Hajdu Kristof Molnar Peter M. Nagy Katalin Sinko Miklos Zrinyi

PII: S0927-7757(16)30355-7
DOI: http://dx.doi.org/doi:10.1016/j.colsurfa.2016.05.036
Reference: COLSUA 20660

To appear in: *Colloids and Surfaces A: Physicochem. Eng. Aspects*

Received date: 2-2-2016
Revised date: 10-5-2016
Accepted date: 11-5-2016

Please cite this article as: Angela Jedlovszky-Hajdu, Kristof Molnar, Peter M.Nagy, Katalin Sinko, Miklos Zrinyi, Preparation and properties of a magnetic field responsive three-dimensional electrospun polymer scaffold, Colloids and Surfaces A: Physicochemical and Engineering Aspects http://dx.doi.org/10.1016/j.colsurfa.2016.05.036

This is a PDF file of an unedited manuscript that has been accepted for publication. As a service to our customers we are providing this early version of the manuscript. The manuscript will undergo copyediting, typesetting, and review of the resulting proof before it is published in its final form. Please note that during the production process errors may be discovered which could affect the content, and all legal disclaimers that apply to the journal pertain.

ACCEPTED MANUSCRIPT

Preparation and properties of a magnetic field responsive three-dimensional electrospun polymer scaffold

Angela Jedlovszky-Hajdu[1], Kristof Molnar[1], Peter M Nagy[2], Katalin Sinko[3], Miklos Zrinyi[1,4]

[1]Laboratory of Nanochemistry, Department of Biophysics and Radiation Biology, Semmelweis University, Nagyvarad tér 4, H-1089 Budapest, Hungary

[2]RCNS-HAS, MEC, Pusztaszeri u. 59-67, 1025, Budapest, Hungary

[3]Institute of Chemistry, L. Eötvös University, Budapest, H-1117, Hungary

[4]Molecular Biophysics Research Group, Hungarian Academy of Sciences, Nagyvarad tér 4, H-1089 Budapest, Hungary

Corresponding author: Angela Jedlovszky-Hajdu, +36-20-666-30-40, hajdu.angela@med.semmelweis-univ.hu, Laboratory of Nanochemistry, Department of Biophysics and Radiation Biology, Semmelweis University, Nagyvarad ter 4, H-1089 Budapest, HUNGARY

ACCEPTED MANUSCRIPT

Graphical abstract

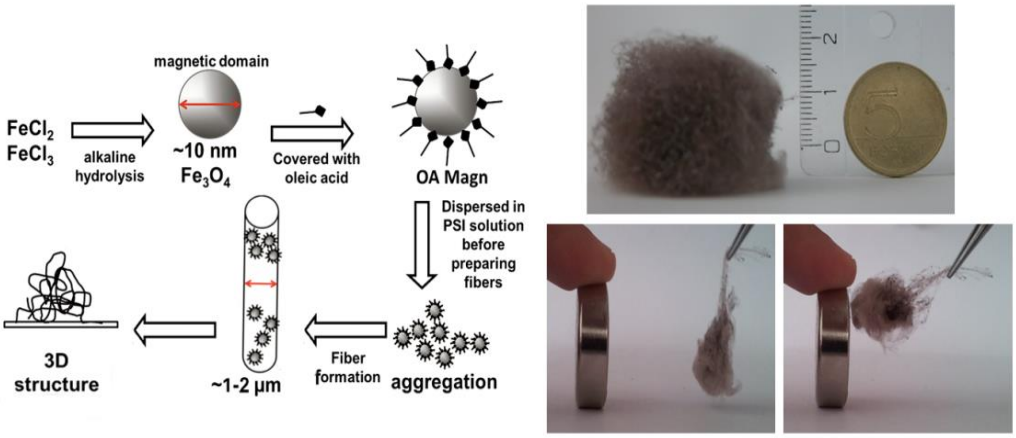

Highlights:

- A new method is reported to prepare 2D and 3D scaffolds by reactive electrospinning
- The prepared scaffolds are magnetic responsive ~~and fully biocompatible~~
- Reactive electrospinning produce non-soluble fibers in the nano scale
- Due to their magnetic character the scaffolds can be used for magnetic hyperthermia

Abstract:

In tissue engineering a permeable 3D fibrous macrostructure with high surface area is desired for cell attachment and growth. In this paper novel experimental technique is reported to prepare 2D and 3D fibrous scaffolds by reactive electrospinning as a potential matrix for cell culturing. The sub-micrometer sized fibrous scaffolds were synthesized from chemically cross-linked poly(succinimide) molecules (anhydrous form of poly(aspartic acid)). Magnetically active particles of what the size distribution was ~~ere~~ determined by small- and wide angle X-ray

ACCEPTED MANUSCRIPT

scatterings were incorporated into the fibers. The morphology of loaded and unloaded fibers was studied by light- and atomic force microscopy. It was found that coupling elastic and magnetic properties within the 3D flexible scaffold enables continuous non-contact mode of mechanical agitation by external magnetic field. These unique properties can be exploited in cell culturing or in magnetic hyperthermia in solid-like matrix.

Keywords: electrospinning, magnetic particles, 3D scaffold, poly(succinimide), magnetic hyperthermia

1. INTRODUCTION

Interest to develop biocompatible and biodegradable polymer matrices has increased recently due to their wide range of applications. In the field of tissue engineering a permeable 3D scaffold with high surface area is required for cell attachment and growth [1]. Electrospinning has recently been the target of many studies because of the sub-micrometer and nanometer sized electrospun fibers that find broad application in multiple biomedical fields.

Poly(amino acid)-based polymers that have desirable chemical, mechanical and biological properties have recently emerged as promising new class of biomaterials [2,3]. In some recent publications preparation of fibrous meshes from biocompatible poly(aspartic acid) (PASP) molecules have been reported [4,5]. However PASP as well as other water soluble fibers prepared by conventional electrospinning techniques may dissolve in bio-relevant media, thus their use is limited in several biomedical fields. In order to prevent dissolution of such polymer

ACCEPTED MANUSCRIPT

matrices, the polymer chains must be bound together in the mesh of fibers [4,6,7]. Electrospinning and cross-linking at the same time requires special technique, named reactive electrospinning where the two processes happen simultaneously [4]. Fiber formation is accompanied by a cross-linking reaction between the polymer molecules resulting in a mesh insoluble in solvents. Cross-linked electrospun polymer meshes can be loaded by magnetic particles. At this procedure the polymer solution is mixed with magnetic fluid prior to electrospinning. Magnetic fluids or ferrofluids, as they are often called, consist of nanosized magnetic particles. In case of superparamagnetic iron oxide nanoparticles the particles are abbreviated as SPION particles [7]. The size of the dispersed particles is controllable in the ranges from a few nanometers up to tens of nanometers. By applying a mixture of polymer solution and magnetic fluids in electrospinning one can obtain magnetic polymer fibers [6,7]. The resulting fibrous mesh amalgamates the unique properties of the magnetism and the elasticity. Beside the appearance of magneto-elastic behavior [8], not only the spatial fiber structure, but also the mechanical properties can be varied in wide range. Due to the presence of magnetic particles not only deformation of mesh can be induced by external magnetic field, but also magnetic hyperthermic effect can be utilized. The first effect is important to enhance the efficiency of cell growth by mechanical agitation, whereas the hyperthermic effect can be used in cancer treatment as an auxiliary therapy beside chemotherapy [9,10]. Realization of a heating effect in solid-like electrospun magnetic scaffold provides novel opportunities [1].

The main purpose of the present work is to prepare magnetic fields responsive electrospun fibers from biocompatible polymers. The chemical procedure is followed by the description of electrospinning process. The effects of process parameters on the fiber morphology are studied by light-, Scanning Electron and Atomic Force Microscope as well as the size of the magnetic domains with small- and wide angle X-ray scattering methods. The demonstration of coupled

ACCEPTED MANUSCRIPT

magnetic and elastic behavior of the electrospun fibers as well as the heating induced by external magnetic field evidence the success of the work.

2. MATERIALS AND METHODS

2.1. Reagents

L-aspartic acid (Sigma-Aldrich, UK), cysteamine (CYSE) (Sigma-Aldrich, UK), dimethyl formamide (DMF) (VWR International, USA), o-phosphoric acid (VWR), iron (II) chloride (VWR International, USA), iron (III) chloride (VWR International, USA), oleic acid (VWR International, USA), sodium-hydroxide (VWR International, USA), acetone (Sigma-Aldrich, UK). All the chemicals were of analytical grade and were used as received.

2.2 Electrospinning

A home-made electrospinning instrument was used to prepare fibers. The instrument includes a syringe pump (KD Scientific KDS100) equipped with a glass needle (Fortuna Optima 7.140-33) as well as a metal Hamilton tip. The 6 and 15 kV voltage was provided by a DC power supply (STATRON TYP4211). One of the electrodes was attached to the metal tip; the other electrode was attached to the collector, made of tinfoil in front of the needle in a well determined distance. The distance between the tip of needle and collector foil was 15 cm. In electrospinning a high voltage is applied to a polymer solution such that charges are induced and a fluid jet releases from the droplet of the tip of the needle and travel towards to a grounded collector. The properties (concentration, viscosity, surface tension, ~~flow rate,~~ etc.) of polymer solution have the most significant influence in the process.

ACCEPTED MANUSCRIPT

2.3 Microscopic techniques (observation)

HUND-WETZLAR H500 light microscope equipped with a Sony Hyper HAD CCD-IRIS/RGB Color Video Camera was used to visualize the samples. For the image analysis Scope Photo software was used. The diameter and surface properties of the polymer fibers were analyzed by Molecular Force Probe 3D (MFP3D) Atomic Force Microscope (AFM) instrument (Asylum Research, Santa Barbara, CA, USA). An OlympusIX81invert microscope was used to fix the target under the AFM tip and oscillation mode was used during the measurements. The dried polymer fibers were measured in air at oscillation mode with resonance frequencies of about 0.2-0.5 Hz and 0.3-0.5 V target value. For the topography pictures 512x512 pixel magnification was used. The axial height distribution along the polymer fiber samples was obtained by manually tracking and then the size distribution was plotted using IgorPro 6 software (Wavemetrics, Lake Oswego, OR). The mean diameters of fibers were determined from 50 randomly selected fibers for each sample.

SEM micrographs of the polymer fibers were taken using a ZEISS EVO 40 XVP scanning electron microscope equipped with an Oxford INCA X-ray spectrometer (EDS). The accelerating voltage of 15-25 kV was applied; the actual voltage was 20 kV in each case. The samples were fixed on a special conductive sticker with tweezers. During the measurements no coating was used, because the conductivity of the samples was high enough to avoid charging of the sample surface.

2.4 Small Angle X-ray Scattering (SAXS) and Wide Angle X-ray Scattering (WAXS)

Simultaneous small-angle and wide-angle X-ray scattering experiments (SAXS and WAXS) were recorded on the JUSIFA beamline of HASYLAB at DESY in Hamburg, using synchrotron radiation source (8 keV photon energy; 925-, and 3625-mm sample-to-detector distances). The

ACCEPTED MANUSCRIPT

SAXS intensities were fitted with a form factor from spheres with a Gaussian size distribution. Wide-angle X-ray scattering were detected with a 1D MYTHEN detector in HASYLAB of DESY (Hamburg). The WAXS data were collected over the 2θ-range of 7-30° with a step size 0.0212°. Identification of phases was achieved by comparing the diffraction patterns with the standard PDF cards.

2.5 Viscosity measurements

Sine-wave Vibro Viscometers (SV-100, A&D Company Ltd, Japan) was used to measure the viscosity of the polymer solutions at room temperature.

2.6 Hyperthermia measurements

A home-made instrument has been used to study the magnetic heating effect due to high frequency magnetic field on the fibrous samples. Alternating magnetic field (AC) was produced in a solenoid coil by a toroid transformer. The measurements were carried out at 60 V with a current of ~~0.~~35 mA. The applied frequency was 88 kHz, and the excited magnetic field was 10.67 kA/m (146.6 Oe). The temperature of the coil was kept constant by a special glass cuvette connected to a thermostat, providing circulating water at room temperature in order to eliminate the effect of self-heating of the coil. The fibrous sample was placed in the middle of the coil horizontally and vertically, respectively. Since the high-frequency magnetic field leads to erroneous temperature measurements in resistance thermometers, we have used infrared thermometer to determine the temperature.

ACCEPTED MANUSCRIPT

3. SYNTHESIS

3.1 Synthesis of poly(succinimide)

Poly(succinimide) abbreviated as PSI was prepared by thermal poly-condensation of L-aspartic acid using phosphoric acid catalyst under high temperature (heat up from room temperature to 180^{o}C) and low pressure (below 10 mbar). The reaction mixture was kept for 7 hours under the above mentioned ~~circumstances~~ conditions, th~~a~~en it was solved in DMF. To remove the unreacted chemicals several washing steps was used. The PSI-DMF mixture was dropped into water and after a 10 min stirring step the polymer was collected with filtering the suspension. The polymer was dried at mild conditions (40^{o}C for 2 days). More detailed description of the preparative process can be found in our previous ~~earlier~~ papers [3,4,11].

3.2 PSI grafted with cysteamine

The chemical structure of PSI chains was modified by grafting cysteamine, in order to bound thiol groups as pendant side chains on the polymer backbone (Fig.1). In a glass reactor cysteamine was added to the PSI-DMF solution and was stirred for an hour. The molar ratio of succinimide monomer units to moles of cysteamine was varied between 10, 15 and 20 respectively ~~respectively~~. This ratio means that - on average – every 10th, 15th and 20th of PSI monomer units bound~~s~~ a cysteamine molecule. The samples are denoted with symbols like 15PSI10CYSE, where the first number stands for the PSI concentration, the second number represents the degree of grafting~~age~~ and CYSE indicate the presence of cysteamine side chain.

ACCEPTED MANUSCRIPT

3.3 Preparation of magnetic nanoparticles and PSI-SPION mixture.

Magnetic nanoparticles (magnetite) were synthesized by alkaline hydrolysis of iron (II) and iron (III) salts and were stabilized by oleic acid monolayer. This surface layer is responsible for the homogenous dispersion of the particles in organic solvents [6,7,12,13].

The particles prepared this way are SPIONs, because each particle carries a single magnetic domain in the nano scale. The particle size, size distribution and characterization have been described in previous publications [12,14].

Magnetite particles were washed with acetone several times, until the supernatant became transparent and all of the unreacted ingredients were removed. Then acetone was evaporated at room temperature. The magnetic particles were dispersed in the polymer solution in different mass concentrations (2.5-10 w%) at high speed stirring for 10 min. The schematic representation of preparative process is shown in Fig2.

In the presence of magnetic nanoparticles, the polymer solution becomes black [6]. The PSI-SPION mixture is identified with symbols like PSI-OAMagn 1, where the last number indicates the sample having magnetite concentration shown in Table I, and OAMagn symbol indicates that the particles were stabilized by oleic acid. Fig. 2 shows the schematic representation of the preparation process.

The viscosity of the base PSI polymer solution without magnetite particles was 1.13 ± 0.0046 Pas (at 25^{o}C). By adding magnetic particles to the system, a significant increase in the viscosity has been found as shown in Table I. This finding is in agreement with the result of [15].

ACCEPTED MANUSCRIPT

To disperse the magnetic particles in the PSI-CYSE polymer solution we faced some difficulties when preparing the system. The oleic acid may not cover completely the nanoparticles, and thus either the free thiol groups on the grafted polymer chain or the amino end groups of the polymer chain can interact with the Fe-OH groups at the surface of the nanoparticles, and cause gelation, during the mixing of components. It is well known that either the thiol or the phosphate group can exchange with the carboxyl group on metal oxide surfaces [16–19]. Therefore a competition takes place between the oleic acid and the cysteamine for the surface Fe-OH groups in our system. Thus the viscosity measurements cannot be implemented because of the fast gelation of the system (details will be explained in the Results and Discussion section and in Table V.).

3.4 Preparation of PSI-SPION composite fibers by reactive electrospinning

In order to prepare stable fibers, hence preventing the polymer chains from dissolution, a cross-linking reaction has to be applied during or after the fiber formation. When cysteamine containing PSI is electrospun in the presence of oxygen e~~nvironment~~, the pendant thiol groups react with each other forming disulphide bonds as shown in Fig.1. [4]. During the electrospinning, the solvent evaporates from the reactive mixture and the chemically cross-linked polymer fibers are deposited on a grounded flat collector like a mesh. The obtained structure is a two or three-dimensional, randomly oriented fiber network in micro- or nano-size range. This structure resembles to the collagen fiber network existing in the natural extracellular matrix [20,21].

We have prepared fibers from both PSI and PSI-SPION composites. The following abbreviation was used to distinguish the samples: PSI-OAMagn x and PSI-CYS-OAMagn x, where x is an

ACCEPTED MANUSCRIPT

integer number, which characterizes the experimental data of electrospinning process given in Tables I - III.

4. Results and Discussion

We have proved that electrospinning is a versatile method to prepare fibers from poly(succinimide) under a fully controllable way. In the following paragraph structure and properties of the electrospun fibers are discussed.

4.1 Structure and morphology of the PSI fibers and mesh

Fig. 3 shows micro- and macrostructure of PSI fibers. In the absence of magnetic nanoparticles the PSI fibers form a white, flat, non-woven mesh as shown in Fig. 3.a.

In the presence of magnetic nanoparticles, not only the polymer solution but also the fibers become dark as shown in Fig. 3.b. The electrospinning procedure may results either in a flat 2D or a fluffy 3D mesh structures. The fiber mesh shown in Fig. 3.b has macroscopic extent in 3 dimensions in contrast to that shown in Fig. 3.a, where the polymer fibers do not contain magnetic particles. PSI fibers without magnetic particles have a tight, randomly oriented, non-woven flat structure. Magnetite loaded fibers - on the contrary – shows 3D structure, when the concentration exceeds a critical value. This finding is in agreement with the theory of Bonino and Yousefzadeh [22,23]. Bonino and coworkers summarized in their paper the potential parameters which can affect the 3D structure formation during the electrospinning, such as solution components, surface of the collector plate, high charge density materials and so on [23]. Yousefzadeh and coworkers suggested a method to deposit the electrospun fibers on a low surface tension solvent to create 3D structured fiber mesh [22]. We assume that in our case the

ACCEPTED MANUSCRIPT

solution components should induce the special structure during the electrospinning procedure as it will be explained in the following paragraphs.

At low magnetite content (PSI-OAMagn1) the produced scaffold is a thin film, as shown in Fig. 4. This structure is very similar to the scaffold prepared from the pure basic polymer (Fig. 3.a); only the magnetic particle content results in a brownish color of the scaffold. By increasing the magnetite concentration (PSI-OAMagn 2 and 3) 3D macrostructures develops as shown in Fig. 3.b. and Fig. 4. The structural change may originate from the enhanced viscosity of the polymer solution. More detailed analysis of the microscopic structure of prepared meshes (see Fig. 5.a-c.) led us to the conclusion, that magnetic particles underwent aggregation (seen as black spots) either on the surface or inside the fibers.

In order to characterize the surface roughness, AFM measurements have been performed. In Fig. 6.a, the phase contrast profile shows an enhanced surface area of the investigated fiber. In contrast to the unloaded PSI fibers, which show up very smooth surface without defects, the magnetite loaded fibers are characterized by rather rough surfaces. The presence of magnetite particles causes grooves of various sizes on the fibers (Fig. 5.b and c). The fibers widened alongside and the surface became rougher (Fig. 6.a), further increasing the surface area. The diameter of the fibers, determined by AFM (1.43 ± 0.5 μm), shows a rather broad distribution (Fig. 6.b), which is likely to be the consequence of the presence of particle aggregates.

In a previous publication we determined the distribution of the base polymer (PSI) and it was arisen 500 ± 60 nm [4].

The large difference in the diameter of the loaded and unloaded fibers comes from the interaction between the magnetic particles, the polymer and the electric field. We assume that these interactions should be responsible for the 3D structure which is in agreement with the ~~of~~ prediction Yousefzadeh [22].

ACCEPTED MANUSCRIPT

Table V. evidences that the relative amount of magnetic particles and the cross-linker (cysteamine) have decisive role in the structure formation. If the cross-linking density is relatively high e.g. every 10^{th} of succinimid unit is cross-linked by cysteamine, then even a small amount of particles (2 w%) induces gelation, which hinders electrospinning. When decreasing the amount of cysteamine cross-links (every 15^{th}) a flat 2D fiber mesh has been obtained even in the presence of both 2 and 4 w% of magnetite concentration. Further increasing the magnetite concentration up to 5 w%, results in 3D structure (see Table V.).

We have compared the surface roughness of cross-linked and uncross-linked polymer based fibers. Fig. 7. a and b show typical AFM pictures of the cross-linked polymer fiber loaded with magnetic particles.

The similar surface properties have been found as it was shown in Fig. 5 and 6. In the presence of the magnetic particles the surface became rough, but the particles have not shown big clots as it was observed without the cross-linkers (Fig. 5 and 6). The average diameter of the fibers was found to be 0.5 ± 0.1 μm (Fig. 7.c).

Our hypothesis concerning the deficiency of the visible aggregated clots along the fibers was mentioned in section 3.3. The surface of the magnetite may not completely be covered by oleic acid, thus, the thiol groups can create chemical bonds with the Fe-OH groups on the surface. Thus, cysteamine has a disaggregation effect in the system. This kind of effect was published earlier in the presence of human serum proteins, which also contain a lot of thiol groups [24].

The average diameter of the PSI-CYS fibers without the magnetic particles was found to be less than 0.1 μm (0.088 ± 0.03 μm) [4], while with magnetic particles it increased to 0.5 ± 0.1 μm. We also found the same effect in the non-cross-linked system, where the diameter raised from 0.5 ± 0.06 μm (PSI) to 1.43 ± 0.5 μm (PSI-OAMagn). It is important to note, that the impact of particles on fibers diameter is higher where there were thiol side chains and cross-linking

ACCEPTED MANUSCRIPT

reaction in electrospinning. The reason should be ~~that~~ the chemical reaction between the particles, the polymer and the cross-linker, but this question is still need to be investigated.

4.2 Colloidal state of magnetic particles in the fibers

In order to determine the magnetic particle size inside the fibers and in the aggregates, SAXS and WAXS measurements have been performed and shown in Fig 8 and 9.

The characteristic size derived from the broad peak is around 6 nm (Fig. 8.a). However, the intensity of the broad peak is independent of the concentration of magnetite particles; the distortion belongs to magnetite (Fig. 9.a). This peak cannot be observed on the curves for pure PSI based polymer fibers (Fig. 8.a). The slope of the linear curves is between -3~~,~~.6 and -3~~,~~.7 in the log-log plot and does not change with magnetite concentration (Fig. 9.a). The slope may be related to the surface of compact, 3D magnetite particles and means 2.4-2.3 surface fractals. The peak at around q = 1 belongs to atomic range (WAXS) rather than supra-molecular range (SAXS) of the structure (Fig. 8.b). This peak does not indicate a characteristic size, it is preferable a diffraction peak which reflects the ordering of magnetite (Fig. 8.b). This aggregation has been verified by small diffraction peaks on the WAXS curves, which are derived from poorly crystalline magnetite (Fig. 9.b).

4.3 PSI-SPION fibers in non-uniform magnetic field

Since the fiber mesh contains magnetic particles, consequently a non-uniform external magnetic field attracts it, ~~and~~ thus deforms the mesh as shown in Fig. 10.

The mechanical stress induced by magnetic interaction may play a decisive role in efficient cell growing [1]. Many studies explaining that a small and controlled mechanical stresses enhance cell proliferation [25–29].

ACCEPTED MANUSCRIPT

4.4 Heating of PSI-SPION fibers by external magnetic field

A significant novel property of the magnetite loaded scaffolds is their thermal response to high-frequency external magnetic field. However, in contrast to magnetic fluids where magnetic nanoparticles can respond to the alternating external magnetic field by both Brown- and Neel relaxation [30,31], in the solid scaffold, where the magnetic particles are captured in the fibers or on the surface of the fibers, the heating effect comes solely from the Neel relaxation. The temperature increase observed in our magnetic hyperthermic measurements (Fig. 11.) is comparable with that reported in the papers of Timko et al and Motoyama et al, in magnetic fluids [1,30,31]. Samal et al [1] published an extremely high heating effect, 18^{o}C/70 s, with magnetic particle loaded gelatin hydrogels.

To compare the results with the magnetic particle doped PSI fibers, 7^{o}C/60 s was detected (Fig. 11.). It is worth to note, that the magnetic content of the gelatin hydrogel was 83 w%, instead of the fiber scaffold where this content was 10 w%. After 10 min the electrospun mesh also reaches this temperature increase published by Samal et al [1]. In clinical application the aim is to increase the temperature above 42^{o}C, which is 5^{o}C higher than the normal body temperature [32]. Thus this electrospun fiber mesh with much lower magnetic particle content should be a suitable candidate for hyperthermic application as Amarjargal et al showed it on a different type of electrospun mesh in their paper [33].

The hyperthermic effect is strongly dependent on the size of the particles, thus it is necessary to determine the particle size not just after the preparation, but after the electrospinning, where particle aggregation can occur.

4.5. Dissolution – importance of the cross-linker

ACCEPTED MANUSCRIPT

The fibers in PSI-OAMagn 3D scaffolds are uncross-linked. Consequently the meshes may be dissolved under physiological conditions (pH 7.5 and 150 mM NaCl). For any biomedical application it is an important criterion that the used scaffold keeps its structure during the application and after serving its purpose it degrades and eliminates from the living system [9,10]. Since PSI dissolves rapidly under physiological condition (less than 16 h - results are shown in Fig. 12.), a chemical cross-linker is necessary to fix its structure and prevent the fibers from dissolution. This is not unfamiliar to the biological system, as the extracellular fibers are built up (such as collagen and reticular fibers) of subunits and cross-links in a similar way [21]. To avoid PSI mesh dissolution we created disulphide bonds as cross-links in our system according to the process described in 3.4. section.

Conclusions:

In this paper an experimental technique is reported to create 3D magnetically responsive scaffolds. The electrospun magnetic field responsive fibers are flexible and dimensionally stable. It was found that the magnetic particles loaded into electrospun scaffolds may provide a unique platform for the design of biomimetic fibrous scaffold for potential cell culturing. The preparation of sub-micrometer sized, two or three dimensional fibrous scaffolds from magnetite doped poly(succinimide) that are cross-linked by cysteamine is a novel approach with great promise in tissue engineering applications.

One important and well known advantage of these fibers is that they provide high surface for cells, leading to a better cell attachment. In the paper it is ~~clearly~~ demonstrated on the microscopic pictures (taken both by AFM and SEM) that the presence of magnetic particles suggests an increase ~~d~~ of the fiber surface. The scaffold thickness for cell growing is usually around 2-5 mm, and one of the most important parameter is the porosity. Sufficient pore size is

ACCEPTED MANUSCRIPT

needed not just for cell migration, but for nutrient transport and for the vascularization [34]. The magnetic nanoparticles dispersed in cysteamine grafted poly(succinimed) results in a special structure in the presence of high voltage. This provides an advantage for using the scaffold for cell growing.

The matrices are built up solely by biocompatible compounds: not only the polymer that turns to poly(amino acid) under physiological conditions but also the magnetic particles which have previously been reported to be biocompatible as well [25,26]. In spite of the biocompatibility test haven't been done yet, the magnetic scaffold is a promising candidate to be biocompatible because of its composition ~~compound~~.

Furthermore, the magnetic character of the meshes allows it~~'~~s selective heating in the presence of alternating magnetic field by means of magnetic hyperthermia. The possibility of using magnetic hyperthermia in such solid meshes is clearly demonstrated here.

Acknowledgement: This research was supported by OTKA K 115259 and OTKA K 105523. The authors would like to thank to Tamás Stirling for the helps in the statistical figures in the AFM measurements.

References:

[1] S.K. Samal, V. Goranov, M. Dash, A. Russo, T. Shelyakova, P. Graziosi, et al., Multilayered Magnetic Gelatin Membrane Scaffolds., ACS Appl. Mater. Interfaces. 7 (2015) 23098–109. doi:10.1021/acsami.5b06813.

[2] G. Hinrichsen, Biomedical polymers, designed-to-degrade systems. Edited by Shalaby W. Shalaby, Hanser Publishers, Munich 1994,263 pp., DM 188.00, ISBN 3-446-16531-2, Acta Polym. 46 (1995) 404. doi:10.1002/actp.1995.010460509.

[3] M. Zrinyi, T. Gyenes, D. Juriga, J. Kim, Acta Biomaterialia Volume change of double cross-linked poly (aspartic acid) hydrogels induced by cleavage of one of the crosslinks

ACCEPTED MANUSCRIPT

Thermal treatment, Acta Biomater. 9 (2013) 5122–5131. doi:10.1016/j.actbio.2012.08.046.

[4] K. Molnar, D. Juriga, P.M. Nagy, K. Sinko, A. Jedlovszky-Hajdu, M. Zrinyi, Electrospun poly(aspartic acid) gel scaffolds for artificial extracellular matrix, Polym. Int. 63 (2014) 1608–1615. doi:10.1002/pi.4720.

[5] C. Zhang, S. Wu, X. Qin, Facile fabrication of novel pH-sensitive poly(aspartic acid) hydrogel by crosslinking nanofibers, Mater. Lett. 132 (2014) 393–396. doi:10.1016/j.matlet.2014.06.031.

[6] I. Savva, G. Krekos, A. Taculescu, O. Marinica, L. Vekas, T. Krasia-Christoforou, Fabrication and Characterization of Magnetoresponsive Electrospun Nanocomposite Membranes Based on Methacrylic Random Copolymers and Magnetite Nanoparticles, J. Nanomater. 2012 (2012) 1–9. doi:10.1155/2012/578026.

[7] L. Vekas, Magnetic nanofluids properties and some applications, Rom. J. Phys. 49 (9-10) (2004) 707–721.

[8] N.M. Wereley, Magnetorheology, The Royal Society of Chemistry, 2014. doi:10.1039/9781849737548.

[9] S. Agarwal, J.H. Wendorff, A. Greiner, Use of electrospinning technique for biomedical applications, Polymer (Guildf). 49 (2008) 5603–5621. doi:10.1016/j.polymer.2008.09.014.

[10] C.H. Kim, M.S. Khil, H.Y. Kim, H.U. Lee, K.Y. Jahng, An Improved Hydrophilicity via Electrospinning for Enhanced Cell Attachment and Proliferation, (2005) 283–290. doi:10.1002/jbmb.

[11] T. Gyenes, V. Torma, B. Gyarmati, M. Zrínyi, Synthesis and swelling properties of novel pH-sensitive poly(aspartic acid) gels., Acta Biomater. 4 (2008) 733–44. doi:10.1016/j.actbio.2007.12.004.

[12] a. Hajdú, E. Illés, E. Tombácz, I. Borbáth, Surface charging, polyanionic coating and colloid stability of magnetite nanoparticles, Colloids Surfaces A Physicochem. Eng. Asp. 347 (2009) 104–108. doi:10.1016/j.colsurfa.2008.12.039.

[13] E. Tombácz, E. Illés, D. Bica, L. Vékás, A. Hajd, Magnetite Nanoparticles Stabilized Under Physiological Conditions for Biomedical Application, (2008) 29–37.

[14] E. Tombácz, D. Bica, a Hajdú, E. Illés, a Majzik, L. Vékás, Surfactant double layer stabilized magnetic nanofluids for biomedical application., J. Phys. Condens. Matter. 20 (2008) 204103. doi:10.1088/0953-8984/20/20/204103.

[15] P.C. Mishra, S. Mukherjee, S.K. Nayak, A. Panda, A brief review on viscosity of nanofluids, Int. Nano Lett. 4 (2014) 109–120. doi:10.1007/s40089-014-0126-3.

[16] F. Dubois, B. Mahler, B. Dubertret, E. Doris, C. Mioskowski, A Versatile Strategy for Quantum Dot Ligand Exchange, J. Am. Chem. Soc. 129 (2007) 482–483. doi:10.1021/ja067742y.

[17] J.C. Love, L. a Estroff, J.K. Kriebel, R.G. Nuzzo, G.M. Whitesides, Self-assembled monolayers of thiolates on metals as a form of nanotechnology., 2005. doi:10.1021/cr0300789.

ACCEPTED MANUSCRIPT

[18] S. Salmaso, P. Caliceti, Stealth properties to improve therapeutic efficacy of drug nanocarriers., J. Drug Deliv. 2013 (2013) 374252. doi:10.1155/2013/374252.

[19] R. Sperling, W.J. Parak, Surface modification, functionalization and bioconjugation of colloidal inorganic nanoparticles., Philos. Trans. A. Math. Phys. Eng. Sci. 368 (2010) 1333–83. doi:10.1098/rsta.2009.0273.

[20] T.G. Kim, T.A.E.G. Park, Biomimicking Extracellular Matrix : Cell Adhesive RGD Peptide Modified Electrospun Poly(D,L-lactic-co-glycolic acid) Nanofiber Mesh, Tissue Eng. 12 (2006) 221–233.

[21] K. Nam, T. Kimura, S. Funamoto, A. Kishida, Preparation of a collagen/polymer hybrid gel designed for tissue membranes. Part I: controlling the polymer-collagen cross-linking process using an ethanol/water co-solvent., Acta Biomater. 6 (2010) 403–8. doi:10.1016/j.actbio.2009.06.021.

[22] M. Yousefzadeh, M. Latifi, M. Amani-tehran, W. Teo, S. Ramakrishna, A Note on the 3D Structural Design of Electrospun Nanofibers, J. Eng. Fiber. Fabr. 7 (2012) 17–23.

[23] C. Bonino, K. Efimenko, S.I. Jeong, M.D. Krebs, E. Alsberg, S. Khan, Three-dimensional electrospun alginate nanofiber mats via tailored charge repulsions., Small. 8 (2012) 1928–36. doi:10.1002/smll.201101791.

[24] A. Jedlovszky-Hajdu, F. Baldelli Bombelli, M.P. Monopoli, E. Tombacz, K.A. Dawson, Surface Coatings Shape the Protein Corona of SPIONs with Relevance to Their Application in Vivo, Langmuir. 28 (2012) 14983–14991. doi:dx.doi.org/10.1021/la302446h.

[25] C. Wilhelm, F. Gazeau, Universal cell labelling with anionic magnetic nanoparticles., Biomaterials. 29 (2008) 3161–74. doi:10.1016/j.biomaterials.2008.04.016.

[26] L.M. Lacava, V. a. P. Garcia, S. Kückelhaus, R.B. Azevedo, N. Sadeghiani, N. Buske, et al., Long-term retention of dextran-coated magnetite nanoparticles in the liver and spleen, J. Magn. Magn. Mater. 272-276 (2004) 2434–2435. doi:10.1016/j.jmmm.2003.12.852.

[27] H. Kurazumi, M. Kubo, M. Ohshima, Y. Yamamoto, Y. Takemoto, R. Suzuki, et al., The effects of mechanical stress on the growth, differentiation, and paracrine factor production of cardiac stem cells., PLoS One. 6 (2011) e28890. doi:10.1371/journal.pone.0028890.

[28] M.K. Jain, R.. Berg, G.P. Tandon, Mechanical stress and cellular metabolism in living soft tissue composites, Biomaterials. 11 (1990) 465–472. doi:10.1016/0142-9612(90)90059-Y.

[29] J. Schimmelpfeng, H. Dertinger, Action of a 50 Hz Magnetic Field on Proliferation of Cells in Culture, 183 (1997) 177–183.

[30] M. Timko, A. Dzarova, J. Kovac, A. Skumiel, A. Józefczak, T. Hornowski, et al., Magnetic properties and heating effect in bacterial magnetic nanoparticles, J. Magn. Magn. Mater. 321 (2009) 1521–1524. doi:10.1016/j.jmmm.2009.02.077.

[31] J. Motoyama, T. Hakata, R. Kato, N. Yamashita, T. Morino, T. Kobayashi, et al., Size dependent heat generation of magnetite nanoparticles under AC magnetic field for cancer therapy., Biomagn. Res. Technol. 6 (2008) 4. doi:10.1186/1477-044X-6-4.

[32] Q. A. Pankhurst, N.T.K. Thanh, S.K. Jones, J. Dobson, Progress in applications of

ACCEPTED MANUSCRIPT

magnetic nanoparticles in biomedicine, J. Phys. D. Appl. Phys. 42 (2009) 224001. doi:10.1088/0022-3727/42/22/224001.

[33] A. Amarjargal, L.D. Tijing, C. Park, I. Im, Controlled assembly of superparamagnetic iron oxide nanoparticles on electrospun PU nanofibrous membrane : A novel heat-generating substrate for magnetic hyperthermia application, Eur. Polym. J. 49 (2013) 3796–3805. doi:10.1016/j.eurpolymj.2013.08.026.

[34] J.C.Y. Dunn, D. Ph, W. Chan, V. Cristini, D. Ph, J.S. Kim, et al., Analysis of Cell Growth in Three-Dimensional Scaffolds, 12 (2006).

Figure Legends

Fig 1. Synthesis and modification of poly(succinimide).

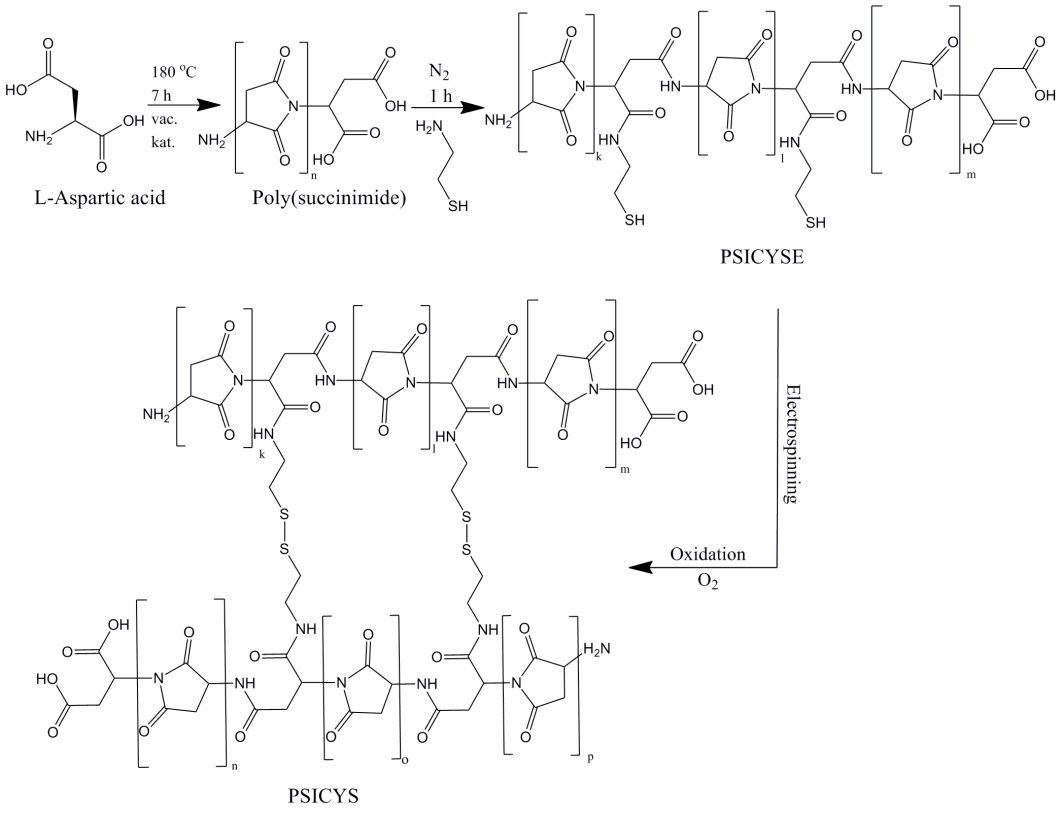

ACCEPTED MANUSCRIPT

Fig. 2. Schematic representation of preparation of magnetite loaded PSI fibers.

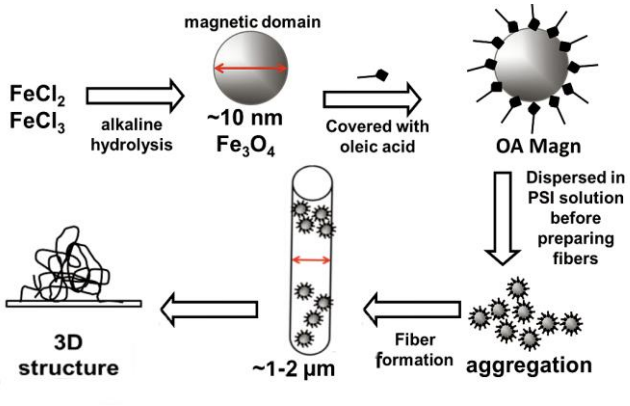

ACCEPTED MANUSCRIPT

Fig. 3. Microscopic and macroscopic structure of electrospun PSI fibers a) mesh of unloaded PSI fibers on the thin collector and seen by light microscope, b) 3D structure of magnetite loaded PSI fibers.

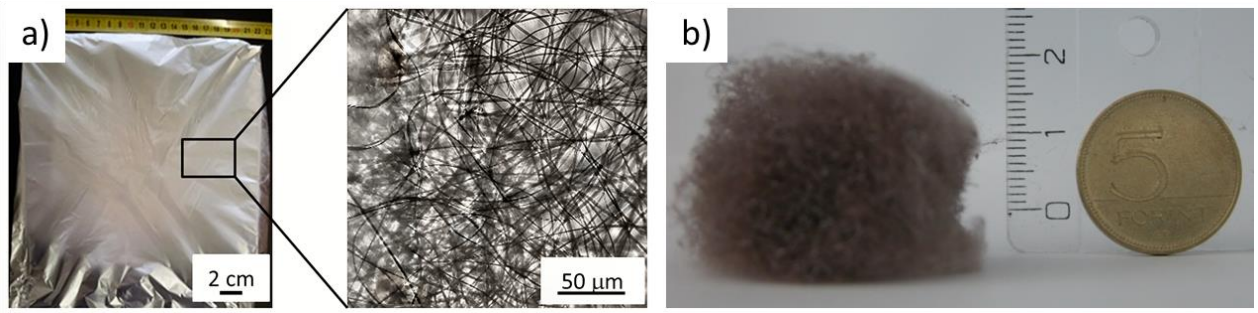

ACCEPTED MANUSCRIPT

Fig. 4. Structural changes of the PSI fiber mesh loaded with different amounts of magnetic nanoparticles.

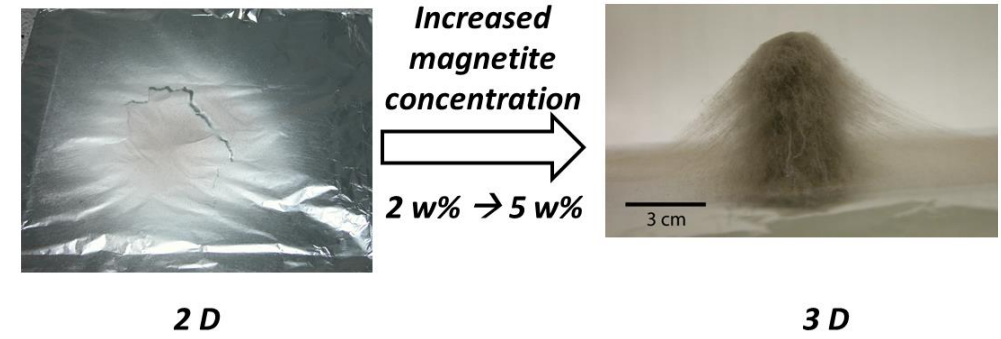

ACCEPTED MANUSCRIPT

Fig. 5. a) The light microscopic, b) the AFM picture and c) SEM picture of the PSI nanofibers loaded with magnetic nanoparticles.

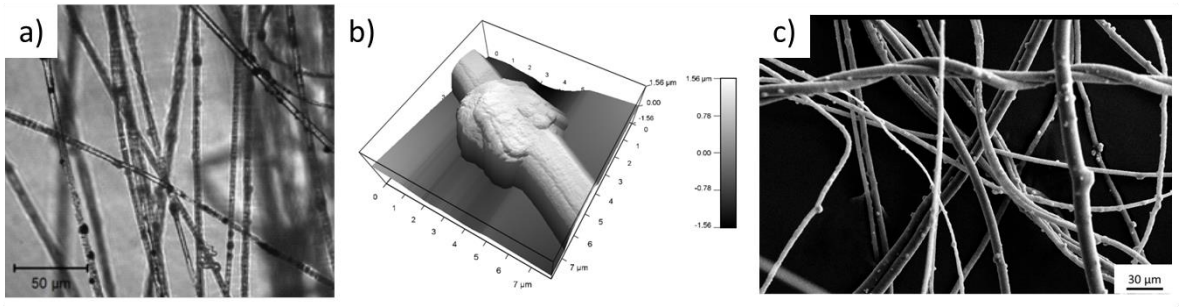

ACCEPTED MANUSCRIPT

Fig. 6. a) Surface roughness and b) size distribution of the PSI fibers loaded with magnetic nanoparticles, measured by AFM. c) SEM pictures of the magnetite loaded mesh.

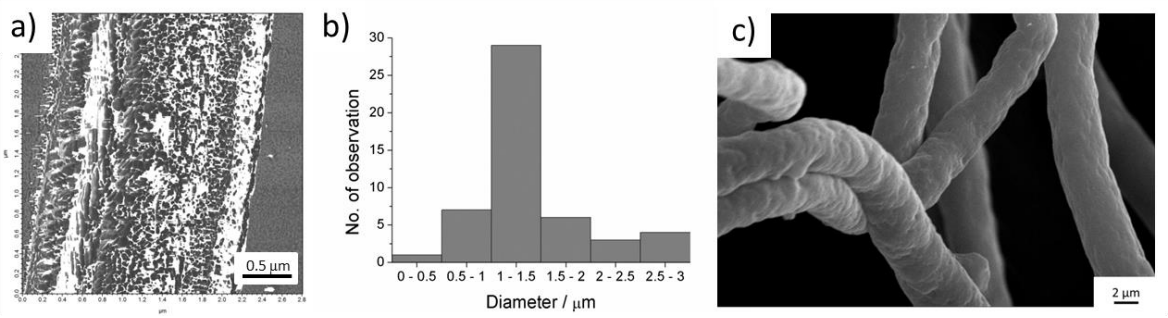

ACCEPTED MANUSCRIPT

Fig. 7. a) Surface roughness, b) inhomogeneity and c) the size distribution of the PSI-CYSE fibers loaded with magnetic nanoparticles.

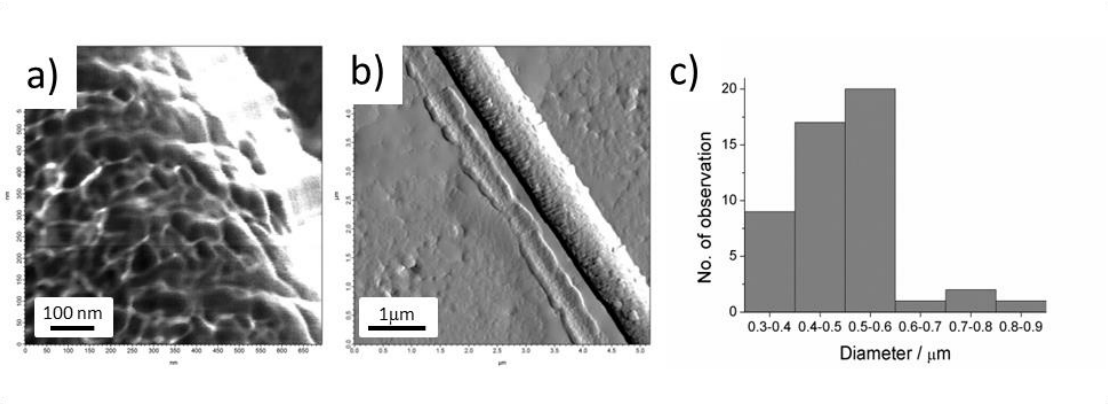

ACCEPTED MANUSCRIPT

Fig. 8. a) SAXS and b) WAXS patterns of the PSI and the PSI-OAMagn3 samples.

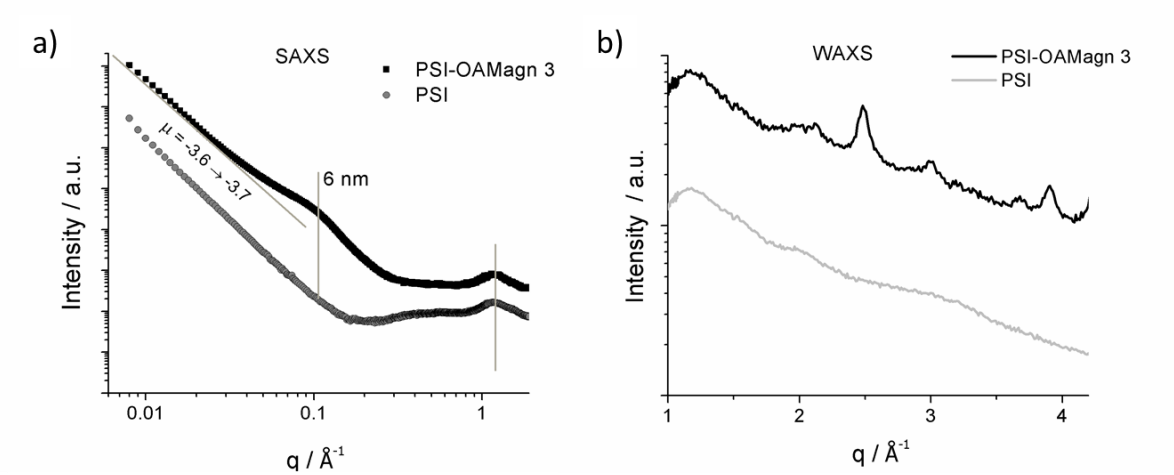

ACCEPTED MANUSCRIPT

Fig 9. a) SAXS and b) WAXS patterns of the PSI-OAMagn samples at different magnetite contents.

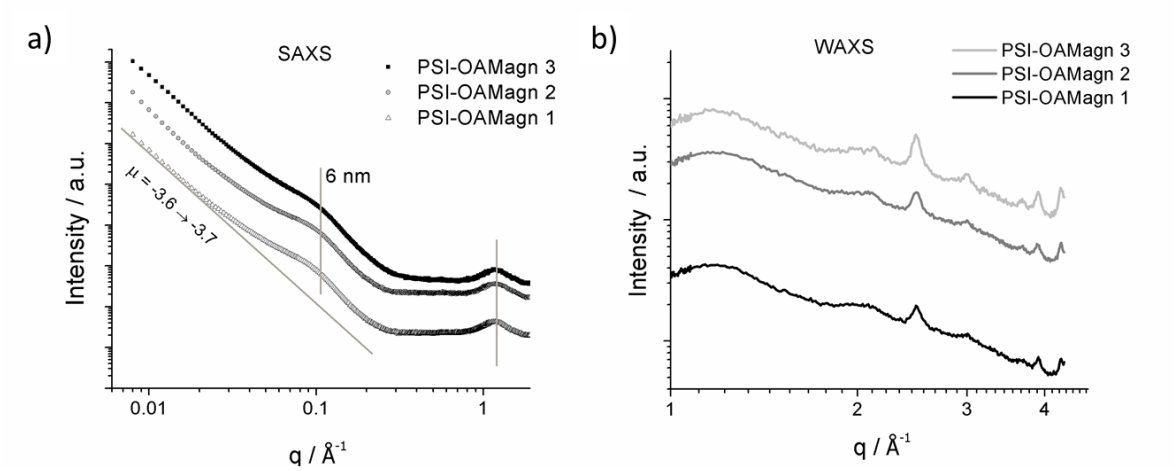

ACCEPTED MANUSCRIPT

Fig. 10. Attraction of electrospun fiber mesh loaded with magnetic particles by non-uniform magnetic field.

ACCEPTED MANUSCRIPT

Fig. 11. Magnetic hyperthermic effect of the magnetite loaded mesh: The temperature change as a function of time for sample PSI-OAMagn 3.

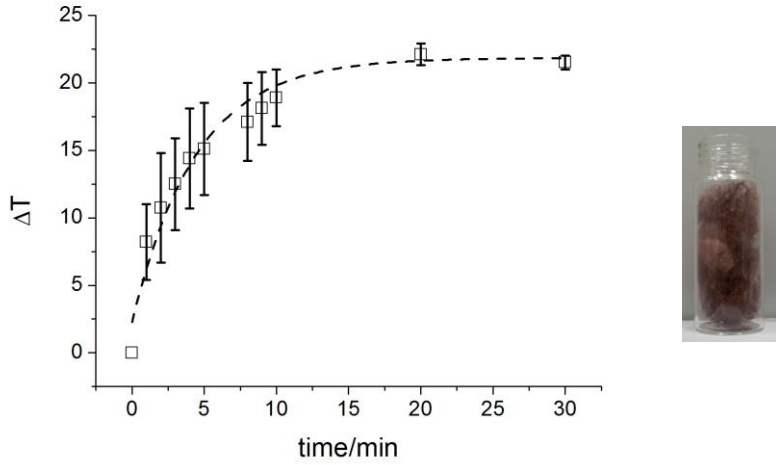

ACCEPTED MANUSCRIPT

Fig. 12. PSI fibrous mesh dissolution at physiological condition in time.

ACCEPTED MANUSCRIPT

List of Tables

Table I. Viscosity of PSI-SPION mixture.

Sample	**Magnetite concentration, w/w %**	**Viscosity (at 25ºC), Pas**
PSI-OAMagn 1	2.5	1.79 ± 0.0051
PSI-OAMagn 2	5	2.92 ± 0.0047
PSI-OAMagn 3	10	7.35 ± 0.0143

ACCEPTED MANUSCRIPT

Table II. Technical parameters of electrospinning process.

Sample	**Magnetite concentration, w/w%**	**Flow rate, ml/h**	**Voltage, kV**
PSI-OAMagn 1	2.5	0.4	6
PSI-OAMagn 2	5	1.2	8-7
PSI-OAMagn 3	10	1.2	8-8.5

ACCEPTED MANUSCRIPT

Table III. Technical parameters of reactive electrospinning process.

Sample	**PSI, w/w% / Grafting number**	**Magnetite concentration, w/w%**	**Flow rate, ml/h**	**Voltage, kV**
PSI-CYS-OAMagn 1	15/10	2	-	-
PSI-CYS-OAMagn 2	15/10	4.6	-	-
PSI-CYS-OAMagn 3	15/15	2	1.2	8
PSI-CYS-OAMagn 4	15/15	4	1.2	10
PSI-CYS-OAMagn 5	15/15	5	1.2	6.5-7

ACCEPTED MANUSCRIPT

Table IV. The influence of solution viscosity on the morphology of electrospun fibers.

Sample	**Magnetite concentration, w/w %**	**Morphology**	**Viscosity (at 25°C), Pas**
PSI-OAMagn 1	2.5	2D thin film	1.79 ± 0.0051
PSI-OAMagn 2	5	3D spiderweb like structure	2.92 ± 0.0047
PSI-OAMagn 3	10	3D spiderweb like structure	7.35 ± 0.0143

ACCEPTED MANUSCRIPT

Table V. Macroscopic changes of PSI-CYSE system at different magnetite and cysteamine concentrations.

PSI w/w% / Grafting number	**Magnetite concentration, w/w %**	**Notes**
15/10	2	Gel formation in the presence of MPs
15/10	4.6	Gel formation in the presence of MPs
15/15	2	Homogenous 2D thin film
15/15	4	Homogenous 2D thin film
15/15	**5**	**Spiderweb like 3D sturcture**